Water-Rock Interactions, Ore Deposits, and Environmental Geochemistry: A Tribute to David A. Crerar
© The Geochemical Society, Special Publication No. 7, 2002
Editors: Roland Hellmann and Scott A. Wood

Corrosion forms and twinning in zeolite ZSM-5 crystals

CLARENCE D. CHANG*#, CYNTHIA T.-W. CHU**, AND JOHN L. SCHLENKER†

Mobil Technology Company, Strategic Research Center, Paulsboro, NJ 08066, USA
*Present address: 11 Murray Place, Princeton, NJ 08540 USA
**Present address: AI Technology, Inc., Princeton Jct., NJ 08550 USA
† deceased

corresponding author (e-mail: cdchang@nji.com)

Abstract—The dissolution (corrosion) of twinned and untwinned zeolite ZSM-5 crystals by carbonate solutions often produces distinctive hollow crystals with the appearance of "open sarcophagi". This phenomenon is examined in light of the distribution of framework aluminum coupled with symmetry constraints imposed by the point-group symmetry of the crystals. The ZSM-5 morphology and possible macroscopic twin laws are also briefly discussed. Dissolution under highly alkaline conditions (1N Na_2CO_3, 90 °C) is incongruent and directional. Scanning electron micrographs show that the carbonate solution selectively attacks the pinacoid form {010}, which comprises (010) and $(0\bar{1}0)$ crystal faces. Incongruent behavior is attributed to the relative corrosion resistance of the {100} and {102} forms, which arises from Al-enrichment at the associated faces. Selective Al-enrichment in this zeolite occurs during crystallization under hydrothermal conditions. The observations provide a basis for some speculations on possible mechanisms of Al incorporation during crystal growth. It is hypothesized that the rate of dissolution is accelerated at regions of high strain energy and retarded at regions of relatively higher Al concentration. Thus, selective dissolution can be seen to initiate at twin boundaries. In contrast, dissolution of untwinned crystals is observed to be more uniform.

1. INTRODUCTION

The synthetic zeolite ZSM-5 (Argauer and Landolt, 1972; Kokotailo et al., 1978) and its recently discovered natural analogue, mutinaite (Galli et al., 1997), are highly siliceous, microporous tectoaluminosilicates. The ZSM-5 structure is a negatively-charged network of four-connected tetrahedra bridged by corner-sharing oxygen atoms charge-balanced by cations situated within the zeolite pore structure. Macroscopic twinning is frequent in synthetic ZSM-5, but is not yet reported for the mineral analog mutinaite. The synthetic material is known to be ferroelastic. Zeolite ZSM-5 has found widespread industrial application due to a unique suite of catalytic and sorptive properties combined with high thermal and hydrothermal stability (Olson et al., 1981).

The dissolution of ZSM-5 in alkaline solutions is incongruent (Čižmek et al., 1994) and directionally non-uniform, often producing hollow crystals with the characteristic appearance of "open sarcophagi", as exemplified in Fig. 1b. This distinctive phenomenon, along with incongruent dissolution, has been linked to "aluminum zoning" (von Ballmoos and Meier, 1981; Derouane et al., 1981; Althoff et al., 1993) in the zeolite crystal. The preferential removal of framework Si was attributed to kinetically-favored base-catalyzed hydrolysis of siloxy bridges, whereas negatively-charged Al centers were assumed to be more resistant to hydroxyl attack (Dessau et al., 1993; Čižmek et al., 1995).

This can be compared to the dissolution behavior of feldspars, a group of commonly-occurring aluminosilicate minerals. Taking albite feldspar as an example, the initial stages of dissolution at 25 °C and at basic pH are characterized by essentially congruent dissolution (Holdren and Speyer, 1985; Chou and Wollast, 1984; Casey et al., 1989). On the other hand, at elevated temperatures (100-300 °C), there is evidence of incongruent dissolution at moderately basic conditions ($r_{Al} > r_{Si}$); this trend is amplified ($r_{Al} >> r_{Si}$) at extremely basic pH conditions and temperatures >200 °C (r = rate of release; see details in Hellmann et al., 1990; Hellmann, 1995).

The present study provides further elaboration of the selective dissolution phenomenon in ZSM-5 zeolite in a crystallographic-morphological context. Several possible reasons for the observed differences in the dissolution behavior of twinned and untwinned ZSM-5 crystals are discussed.

2. COMPOSITION AND STRUCTURE OF ZSM-5 ZEOLITE: EXPERIMENTAL METHODS

The ZSM-5 (MFI framework) structure is characterized by a 10-ring system of interpenetrating channels. A sinusoidal channel parallel to the a-axis has

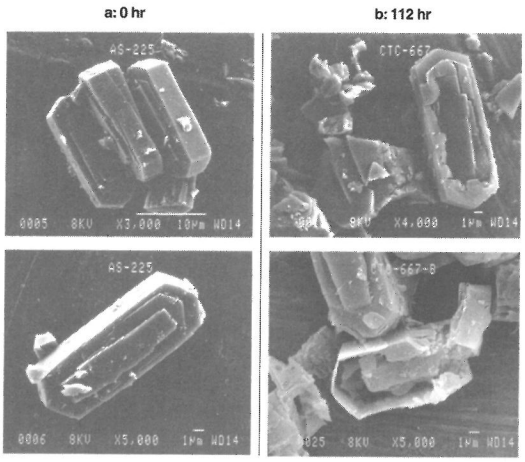

Fig. 1: Scanning electron micrographs of macroscopically twinned ZSM-5 crystals (Si/Al = 110) before and after alkaline treatment

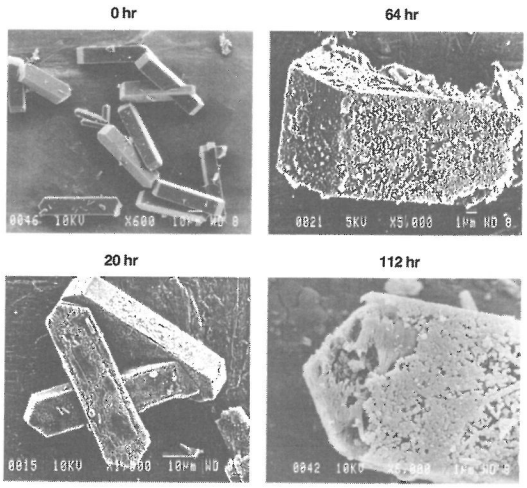

Fig. 2: Scanning electron micrographs of untwinned ZSM-5 crystals (Si/Al = 1500) during alkaline treatment

dimensions 5.1 × 5.5 Å and a second linear channel, parallel to the b-axis, is 5.3 × 5.6 Å (Olson et al., 1981). The crystal structure (framework topology) of ZSM-5 is characterized by a large number of five-membered rings, but there is also a small fraction of four-membered rings. The ideal unit cell formula is represented by $M_{x/n}(AlO_2)_x(SiO_2)_{96-x}\cdot zH_2O$, where M is a cation of valence *n*. Occluded water may be replaced by various organic substances. The composition is highly variable, but ZSM-5 with end-member composition (x = 0) $Si_{96}O_{192}$ is readily synthesized.

Crystals of zeolite ZSM-5 were synthesized with Si/Al 110 and 1500 following published procedures (Argauer and Landolt, 1972). The as-synthesized zeolite crystals were air-calcined to remove the tetrapropylammonium directing agent, and digested (in stainless steel Parr® autoclaves under static conditions) with excess aqueous 1N Na_2CO_3 at 90 °C for varying lengths of time up to 112 hr. Samples of the crystals were periodically removed, washed with deionized water, dried, and examined with a scanning electron microscope (SEM).

3. RESULTS

Scanning electron micrographs of zeolite crystals before and after alkali treatment (up to 112 hr) are shown in Figs. 1 and 2. Figure 1 shows results for twinned crystals, whereas Fig. 2 shows results for untwinned crystals. Selective etching-dissolution is most prominent in the macroscopically twinned crystals (Fig. 1b). These samples also show evidence of accelerated, possibly discontinuous, dissolution along the twin boundary. In contrast, the results of alkaline treatment of the untwinned crystals, displayed in Fig. 2, show their progressive dissolution at 0, 20, 64, and 112 hr. Here the process appears somewhat slower and more uniform, though incipient selective etching-dissolution is visible at 20 hr. There is also evidence of secondary nucleation on the crystal surface at 64-112 hr. The morphology of these exterior crystals, coupled with their generation presumably by a seeding mechanism (Ostwald ripening) or epitaxy, indicate that they are ZSM-5 zeolite, though their compositions were not directly analyzed.

4. DISCUSSION

4.1. Mechanism of Alkaline Dissolution

On the basis of kinetic studies, Čižmek et al. (1994) concluded that the alkaline dissolution of ZSM-5 involves at least three main steps: (i) breaking of Si-O-Si and Si-O-Al bonds, with production of silicate and aluminate monomers in solution; (ii) formation of an amorphous SiO_2 layer on the crystal surface by reaction of silicate anions; (iii) dissolution of the amorphous SiO_2. We assume that the reaction initiates at the silanols on the crystal surface. These can be terminal (non-acidic) I, or bridging (acidic) II:

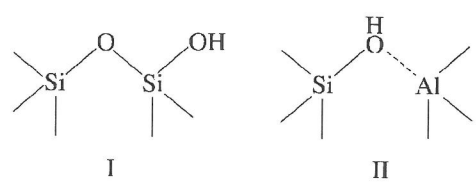

I II

For a working model of the initiation reaction, the mechanism of Dove and Crerar (1990) for quartz dissolution appears reasonable (see also Xiao and Lasaga, 1996, for a quantum mechanical treatment). Dove and Crerar observed dramatic enhancement of the dissolution rate upon addition of small concentrations of alkali cations, even at near-neutral pH conditions. A transition state interpretation (Lasaga, 1981) was invoked, where the activation entropy is increased by surface-coordinated cations, which in turn increases the frequency of species crossing the activated barrier associated with Si-O bond breakage. Given the elevated pH, 1N Na_2CO_3 solutions used in the present study, zeolitic protons (those associated with the bridging siloxyl groups II) will be essentially completely exchanged for Na^+ at equilibrium.

The influence of Al centers in the selective dissolution of ZSM-5 may be given two functionally equivalent interpretations: (*i*) Al centers may be regarded as strongly adsorbed "impurities" (a particularly apt model for the highly siliceous zeolites of this study), which may serve as rate inhibitors (Lasaga, 1997) by virtue of their low reactivity; (*ii*) Al centers (T-sites, II) have higher surface energy due to steric and electronic differences with respect to their neighboring Si T-sites, and serve therefore as "active sites" for initiating silica dissolution. The selective dissolution of minerals at active sites has been extensively investigated (for examples in the geochemistry literature, see e.g., Blum and Lasaga, 1987; Schott et al., 1989).

The marked difference in dissolution behavior between the twinned and untwinned crystals may be attributed to a number of factors, including surface area and Al content. A further consideration is based on differences in surface strain energy. According to Schott et al. (1989), the net surface reaction-limited rate of dissolution r of a flat crystal may be expressed as follows:

$$r = \prod_i a_i^{n_i} \left[\nu \left\{ \sum_{\text{perfect surface sites}} \exp\left(\frac{-\Delta G_p^+}{kT} \right) + \sum_{\text{dislocation surface sites}} \exp\left(\frac{-\Delta G_d^+}{kT} \right) \right\} \right] \quad (1)$$

Here a_i and n_i are the activity and reaction order of the ith species, ν is a frequency factor, and k is the Boltzmann constant. The difference between ΔG_p^+, the activation energy for dissolution of the perfect crystal surface, and that of a surface with dislocations, ΔG_d^+, is the strain energy u associated dislocations. Thus, for a single dislocation, the ratio of the dissolution rate constants for a perfect crystal k_p and a crystal with dislocations k_d can be written:

$$k_p / k_d = exp\,(-u / kT) \quad (2)$$

Referring to the selective dissolution of twinned crystals shown in Fig. 1b, it appears that twinning makes the twin plane surfaces more susceptible to dissolution. Theoretically, a perfectly coherent boundary associated with twinning should not be the locus of any additional strain. However, in reality, it is commonly observed that twin boundaries are areas that are preferentially attacked in solutions; in fact, preferential etching of twin boundaries is a well known method for delimiting twin boundaries (see examples in Heiman et al., 1975; and references therein). Thus, it remains an open question as to whether twinning itself results in elevated strain at the twin boundaries in ZSM-5 crystals.

If twinning is not directly responsible, it is possible that elevated impurity concentrations at twin boundaries are a possible mechanism for increasing the strain energy. Studies on the incorporation of trace elements on mineral surfaces have revealed the complex nature of how surface structure and the kinetic behavior of surface processes strongly affect elemental partitioning (e.g., Paquette and Reeder, 1995; Rakovan and Reeder, 1994; Reeder, 1996). In the case of ZSM-5, Al may play the role of an impurity which is preferentially incorporated at the twin boundary, thereby increasing the strain energy.

Even though Al is known for its role as a dissolution-inhibitor, this effect may be offset by the subsequent increase in the strain energy due to preferential Al incorporation. The net effect would be a higher rate of dissolution along the twin boundaries. In view of Eqns. 1 and 2, the more "perfect" untwinned crystals would be expected to dissolve at a relatively slower rate.

Because the exact nature of the twin boundary in ZSM-5 is not known, another possible reason (E. Dowty, private communication) for the increased rates of dissolution of twinned ZSM-5 crystals may be due to an irregular contact surface associated with interpenetrative twins (in contrast to contact twins, such as albite feldspar twins). Thus, the twin contact surface may be composed of multiple reentrants (alternating {100} and {010} surfaces), which are not present on single crystals. Multiple reentrants have been implicated in influencing crystal growth rates, and therefore, it is possible that they also influence dissolution rates.

4.2. Symmetry and Morphology of ZSM-5 Crystals

ZSM-5 is ferroelastic with a high temperature orthorhombic, o-form, and a low temperature monoclinic, m-form. The ferroelastic transition temperature

Table 1. Symmetry distinct morphological forms of the orthorhombic bipyramidal class (2/m 2/m 2/m)

Form Designation	Designation	Number of Faces	Present on ZSM-5	ZSM-5 form
bipyramid	{hkl}	8	no	-------
a-dome	{h0l}	4	yes	{102}
b-dome	{0kl}	4	yes	{012}
prism	{hk0}	4	no	-------
front-pinacoid	{100}	2	yes	{100}
side-pinacoid	{010}	2	yes	{010}
basal pinacoid	{001}	2	no	-------

is near room temperature and is influenced by both the Si/Al ratio and by applied mechanical stress.

The space group symmetry of o-ZSM-5 is P 2_1/n 2_1/m 2_1/a. The real symmetry of the high temperature or o-form of ZSM-5 coincides with the maximum topological symmetry (MTS) of the aluminosilicate framework. Space group P 2_1/n 2_1/m 2_1/a is isogonal with the centrosymmetric point group 2/m 2/m 2/m . This is a point group of the orthorhombic crystal system traditionally designated the orthorhombic bipyramidal class. A tabulation of forms for this point group symmetry is given in Table 1.

The general {hkl} form (bipyramid) of the orthorhombic bipyramidal crystal class has never been observed with ZSM-5 crystals. For ZSM-5, the dominant morphological forms are the front- and side-pinacoids: {100} and {010}, and the dome {102}. The typical ZSM-5 crystal habit is illustrated in Fig. 3. The ZSM-5 crystal morphology is a result of the appearance of three distinct (symmetrically non-equivalent) forms. These forms appear in combination, because no one form has sufficient faces to enclose space. Symmetrically equivalent faces belonging to each of the three forms are stippled in Fig. 3. The habit of

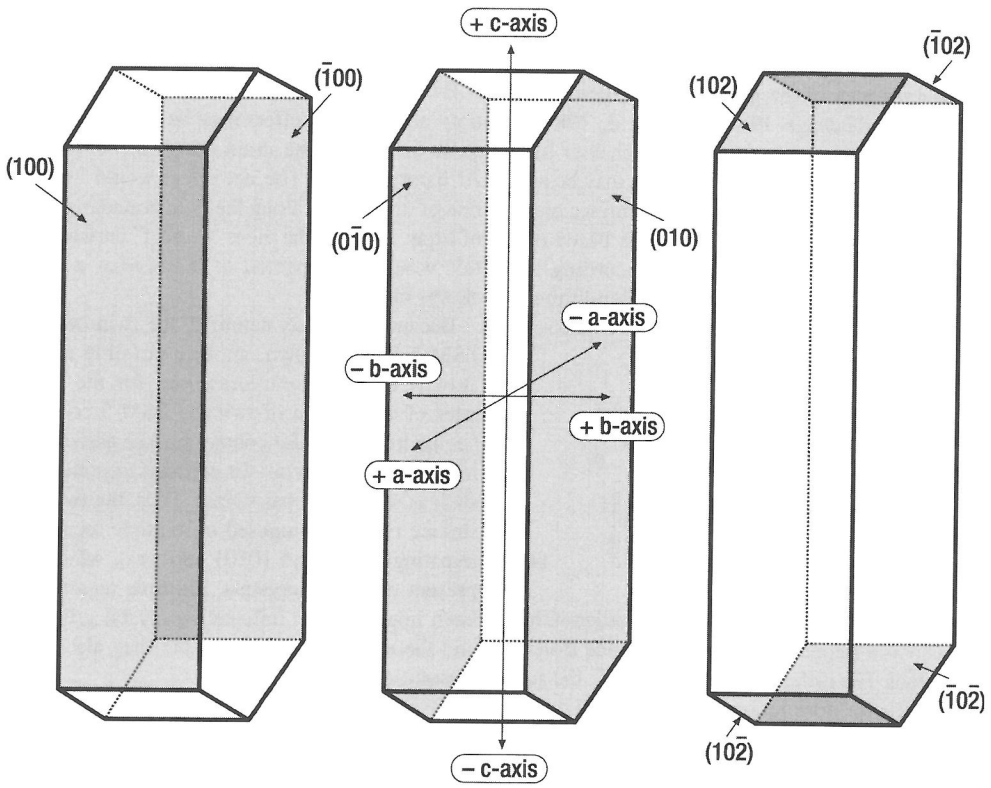

Fig. 3: Crystal habit of ZSM-5 typically exhibits three morphological forms; these are, from left to right, the front-pinacoid, the side-pinacoid, and the a-dome.

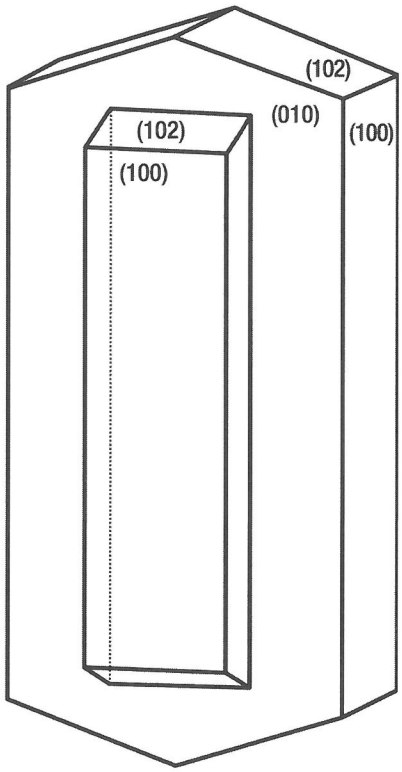

Fig. 4: Typical appearance of a macroscopically-twinned crystal of ZSM-5

ZSM-5 is not always the same since the relative development of the symmetrically distinct morphological forms is variable within limits and can be influenced by the conditions prevailing during crystal growth.

4.3. Macroscopic Twinning and the Twin Law in ZSM-5

In macroscopic twinning, the individuals constituting the twin are related by symmetry transformation operators not formally present in the point group symmetry of the crystal. This form of twinning is favored by the presence of pseudo-symmetry axes and pseudo-mirror planes, and the presence of such pseudo-symmetry axes and pseudo-mirror planes is often indicated by the near equality of two or more symmetry-independent cell parameters of a material. In ZSM-5: a = 20.022 Å and b = 19.899 Å.

In ZSM-5, individual macroscopic twins appear to be related by a 180° rotation about [110]. The usual appearance of such twins is illustrated in Fig. 4. The precise nature of the twin boundary is unclear. Scanning electron micrographs demonstrate that macroscopic twinning is ubiquitous in many, but by no means all, ZSM-5 preparations. Some preparations contain relatively few macroscopically twinned crystals, as untwinned ZSM-5 crystals are not a rarity. Although the ferroelastic transition is immediately detectable using x-ray powder diffraction, there is no obvious difference between powder diffraction patterns of ZSM-5 preparations consisting primarily of macroscopically twinned crystallites and batches where this macroscopic twinning is relatively infrequent. Macroscopic twinning, of course, has presented difficulties for single crystal x-ray diffraction studies.

4.4. Symmetry Information from Dissolution Forms of ZSM-5

The mode of dissolution of ZSM-5 allows us to make certain inferences regarding its habit. The dissolution forms observed here definitely establish that the faces of the principle zone of ZSM-5 cannot belong to a single prismatic {110} form, for, if such were the case, all four faces in this zone should be symmetrically equivalent and react at an equivalent rate. The implication is that the four faces of this prism-like zone are equivalent in pairs and belong to two distinct morphological (pinacoidal) forms, the front-pinacoid {100} and the side pinacoid {010}. It is the faces of the {010} form, that is faces (010) and $(0\bar{1}0)$, that are rapidly attacked during dissolution in the Na_2CO_3 solution. These are the faces opening on the straight zeolite channel. Symmetry theory tells us that because faces (010) and $(0\bar{1}0)$ belong to the same form, they must interact with the solvent in an equivalent way. The two faces of the {100} form, (100) and $(\bar{1}00)$, are observed to be corrosion-resistant. The {102} form is also resistant to corrosion. Because three distinct forms commonly appear on ZSM-5 crystals, three different dissolution rates must be involved; however symmetry theory makes no statement regarding the extent to which these rates should differ. An idealized depiction of the effect of selective dissolution appears in Fig. 5.

The observed habit of ZSM-5 is frequently slightly platy with predominant development of the {010} pinacoid. This habit suggests that after a certain point in their crystallization history ZSM-5 crystals grow primarily by accretion of material to the {100} side-pinacoid and {102} dome faces. Addition of material to the faces of the {010} pinacoid seems to slow or cease. This development may be connected to Si depletion of the surrounding solution and could constitute a clue as to the way in which Al is incorporated into ZSM-5 during growth. As a result of this mode of growth, the {100} and {102} faces should be uniformly Al-enriched (presumably to different extents,

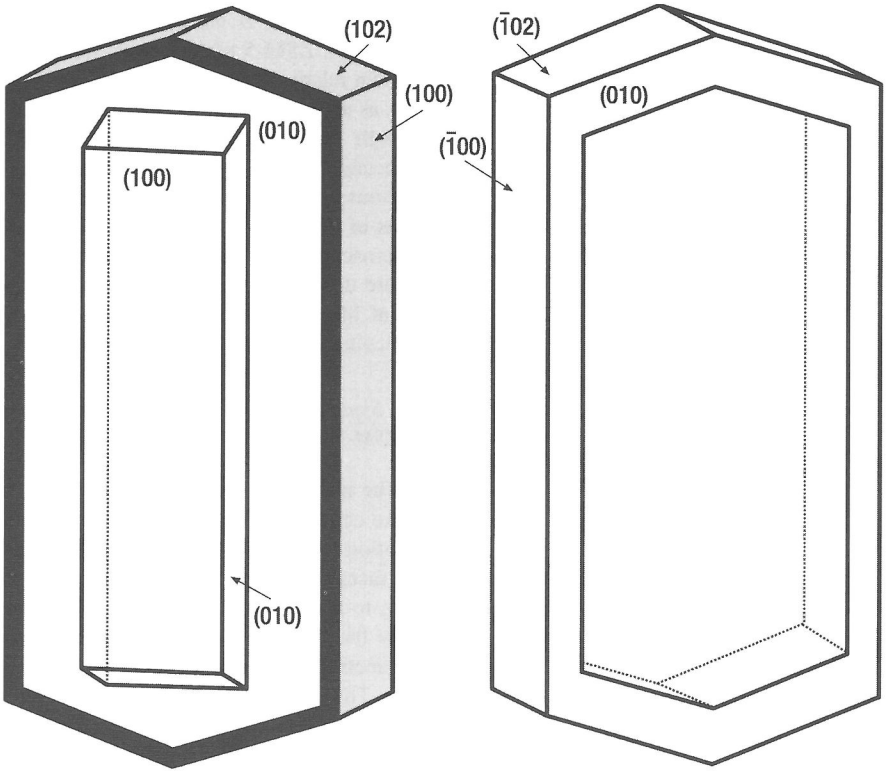

Fig. 5: Idealized depiction of a macroscopically-twinned crystal of ZSM-5 before (on right) and after dissolution (on left) in Na_2CO_3 solution. The aluminum enriched rim is stippled in the left portion of the figure.

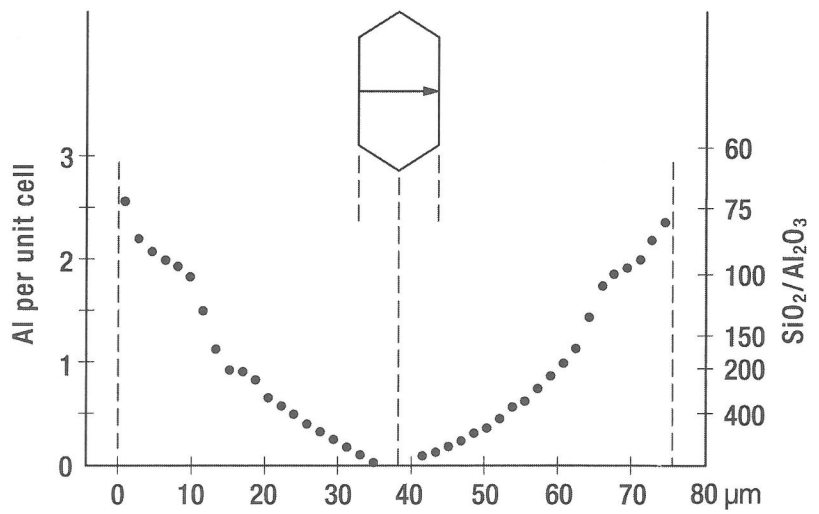

Fig. 6: Al-zoning in a ZSM-5 crystal as revealed through electron microprobe scan (von Ballmoos and Meier, 1981). Reprinted by permission from *Nature* 1998, Macmillan Magazines, Ltd.

since they are symmetrically nonequivalent) and evidently corrosion-resistant. Corrosion resistance is clearly associated with elevated Al concentration. The aluminum incorporation on the crystal faces of the {100} and {102} forms appears compositionally uniform. Corrosion rates must differ for the {100} and {102} forms, but this difference is evidently small.

As demonstrated in Fig. 6 (von Ballmoos and Meier, 1981), the mode of crystal growth described above causes faces of the slowly accreting {010} pinacoidal form to exhibit Al zoning, where the {010} pinacoid faces have a Si-enriched and reactive inner core and an Al-enriched and corrosion resistant outer rim. Curiously, in certain instances the composition change at the core/rim composition boundary appears rather sharp and possibly discontinuous.

5. CONCLUSIONS

The dissolution of macroscopically twinned and untwinned ZSM-5 crystals in Na_2CO_3 solutions shows a directional dependence. In addition, dissolution proceeds more rapidly in macroscopically twinned crystals. A consequence of this behavior is the production of distinctive hollow crystals shaped like "open sarcophagi". This directional solubility is tied to symmetry constraints imposed by the point-group symmetry of the crystals. Scanning electron micrographs demonstrate that the carbonate solution selectively attacks the pinacoid form {010}, which comprises (010) and ($0\bar{1}0$) faces, of the ZSM-5 crystals. The relative corrosion resistance of the {100} and {102} forms is associated with Al-enrichment of these faces during their hydrothermal synthesis. In some crystals, dissolution reveals a sharp core/rim boundary suggesting that the difference in solubility rates is discontinuous. It is hypothesized that dissolution is governed by the interplay of opposing factors, namely surface strain energy, local Al concentration, and dissolution rate retardation by Al. The rate of dissolution is accelerated at regions of high strain energy at twin boundaries, and retarded at regions of relatively higher Al concentration. In contrast, dissolution of untwinned crystals is seen to be more uniform.

Acknowledgments—The authors express their appreciation to R. Hellmann, D. Bosbach, E. Dowty, and H. Teng for constructive comments. John Schlenker, co-author of this paper, passed away on September 20, 2000. Dr. Schlenker was an eminent crystallographer, and was writing a book on the theory of x-ray powder diffraction before his untimely death. David Crerar was a treasured friend of CDC's, who still misses his intellectual fervor and inspiration, as well as the many gastronomical adventures shared through the years.

Editorial handling: R. Hellmann

REFERENCES

Althoff R., Schultz-Dobrick B., Schüth F., and Unger K. (1993) Controlling the spatial distribution of aluminum in ZSM-5 crystals. *Microporous Mater.* **1**, 207-218.

Argauer R. J. and Landolt G. R. (1972) Crystalline zeolite ZSM-5 and method of preparing the same. *U. S. Patent* 3702886.

Blum A. E. and Lasaga A. C. (1987) Monte Carlo simulations of surface reaction rate laws. In *Aquatic Surface Chemistry: Chemical Processes at the Particle-Water Interface* (ed. W. Stumm). John Wiley & Sons, Inc., New York. pp. 255-292.

Casey W. H., Westrich H. R., Arnold G. W., and Banfield J. F. (1989) The surface chemistry of dissolving labradorite feldspar. *Geochim. Cosmochim. Acta* **53**, 821-832.

Chou L. and Wollast R. (1984) Study of the weathering of albite at room temperature and pressure with a fluidized bed reactor. *Geochim. Cosmochim. Acta* **48**, 2205-2217.

Čižmek A., Komunjer L., Subotic B., Aiello R., Crea F., and Nastro A. (1994) Kinetics of zeolite dissolution: Part 4. Influence of the concentration of silicon in the liquid phase on the kinetics of ZSM-5 dissolution. *Zeolites* **14**, 182-189.

Čižmek A., Komunjer L., Subotic B., Aiello R., Crea F., Nastro A., and Tuoto C. (1995) Dissolution of high-silica zeolites in alkaline solutions I. Dissolution of silicalite-1 and ZSM-5 with different aluminum content. *Microporous Mater.* **4**, 159-168.

Derouane E. G., Detremerrie S., Gabelica Z., and Blom N. (1981) Synthesis and characterization of ZSM-5 type zeolites I. Physico-chemical properties of precursors and intermediates. *Appl. Catal.* **I**, 201-224.

Dessau R. M., Valyocsik E. W., and Goeke N. H. (1993) Aluminum zoning in ZSM-5 as revealed by selective silica removal, *Zeolites* **12**, 776 – 779.

Dove P. M. and Crerar D. A. (1990) Kinetics of quartz dissolution in electrolyte solutions using a hydrothermal mixed flow reactor. *Geochim. Cosmochim. Acta* **54**, 955-969.

Galli E., Vezzalini G., and Quartieri S. (1997) Mutinaite, a new zeolite from Antarctica: the natural counterpart of ZSM-5. *Zeolites* **19**, 318–322.

Heiman R. B. (1975) *Auflösung von Kristallen*. Springer-Verlag, Wien.

Hellmann R. (1995) The albite-water system Part II. The time-evolution of the stoichiometry of dissolution as a function of pH at 100, 200 and 300 °C. *Geochim. Cosmochim. Acta* **59**, 1669-1697.

Hellmann R., Eggleston C. M., Hochella M. F., and Crerar D. A. (1990) The formation of leached layers on albite surfaces during dissolution under hydrothermal conditions. *Geochim. Cosmochim. Acta* **54**, 1267-1281.

Holdren G. R. Jr. and Speyer P. M. (1985) Reaction rate-surface area relationships during the early stages of weathering- **I**. Initial observations. *Geochim. Cosmochim. Acta* **49**, 675-681.

Kokotailo G. T., Lawton S. L., Olson D. H., and Meier W. M. (1978) Structure of synthetic ZSM-5. *Nature* **272**, 437-438.

Lasaga A. C. (1981) Transition state theory. In *Kinetics of Geochemical Processes* (eds. A. C. Lasaga and R.J. Kirkpatrick), Reviews in Mineralogy **8**, Mineralogical Society of America, Washington, D.C. pp. 135-169.

Lasaga A. C. (1997) *Kinetic Theory in the Earth Sciences*, Princeton University Press, Princeton.

Olson D. H., Kokotailo G. T., Lawton S. L., and Meier W. M.

(1981) Crystal structure and structure-related properties of ZSM-5. *J. Phys. Chem.* **85**, 2238-2243.

Paquette J. and Reeder R. J. (1995) Relationship between surface structure, growth mechanism, and trace element incorporation in calcite. *Geochim. Cosmochim. Acta* **59**, 735-749.

Rakovan J. and Reeder R. J. (1994) Differential incorporation of trace elements and dissymmetrization in apatite: The role of surface structure during growth. *Amer. Mineral.* **79**, 892-903.

Reeder R. J. (1996) Interaction of divalent cobalt, zinc, cadmium, and barium with the calcite surface during layer growth. *Geochim. Cosmochim. Acta* **60**, 1543-1552.

Schott J., Brantley S., Crerar D., Guy C., Borcsik M., and Willaime C. (1989) Dissolution kinetics of strained calcite, *Geochim. Cosmochim. Acta* **53**, 373-382.

von Ballmoos R. and Meier W. M. (1981) Zoned aluminum distribution in synthetic zeolite ZSM-5, *Nature* **289**, 782 – 783.

Xiao Y. and Lasaga A. C. (1996) Ab initio quantum mechanical studies of the kinetics and mechanisms of quartz dissolution. *Geochim. Cosmochim. Acta* **60**, 2283-2295.